REFERENCES

1. R. Kouyoumjian and P. Pathak, A uniform geometrical theory of diffraction for an edge in a perfectly conducting surface, Proc IEEE 62 (1974), 1448–1461.
2. T. Senior and J. Volakis, Approximate boundary conditions in electromagnetics, IEE Electromagn Wave Series, London, England, 1995.
3. R. Luebbers, A heuristic UTD slope diffraction coefficient for rough lossy wedges, IEEE Trans Antennas Propag 37 (1989), 206–211.
4. P. Holm, A new heuristic UTD diffraction coefficient for nonperfectly conducting wedges, IEEE Trans Antennas Propag 48 (2000), 1211–1219.
5. M. Aïdi and J. Lavergnat, Comparison of Luebbers' and Maliuzhinets' wedge diffraction coefficients in urban channel modelling, Progr Electromagn Res 33 (2001), 1–28.
6. P. Bernardi, R. Cicchetti, and O. Testa, A three-dimensional UTD heuristic diffraction coefficient for complex penetrable wedges, IEEE Trans Antennas Propag 50 (2002), 217–224.
7. H. El-Sallabi and P. Vainikainen, Improvements to diffraction coefficient for non-perfectly conducting wedges, IEEE Trans Antennas Propag 53 (2005), 3105–3109.
8. D. Schettino, F. Moreira, K. Borges, and C. Rego, Novel heuristic UTD coefficients for the characterization of radio channels, IEEE Trans Magn 43 (2007), 1301–1304.
9. J. Whitteker, Measurements of path loss at 910 MHz for proposed microcell urban mobile systems, IEEE Trans Vehicular Technol 37 (1988), 125–129.
10. D. Schettino, F. Moreira, and C. Rego, Efficient ray tracing for radio channel characterization of urban scenarios, IEEE Trans Magn 43 (2007), 1305–1308.

COUPLED-FED LOOP ANTENNA WITH BRANCH RADIATORS FOR INTERNAL LTE/WWAN LAPTOP COMPUTER ANTENNA

Kin-Lu Wong and Pei-Ji Ma
Department of Electrical Engineering, National Sun Yat-sen University, Kaohsiung 80424, Taiwan; Corresponding author: wongkl@ema.ee.nsysu.edu.tw

Received 21 March 2010

ABSTRACT: *A new antenna structure of internal long-term evolution/wireless wide area network (698–960/1710–2690 MHz) laptop computer antenna formed by a coupled-fed loop antenna connected with two branch radiators is presented. The two branch radiators consist of one longer strip and one shorter strip, both being efficient radiators and contributing multiresonant modes to greatly enhance the bandwidth of the antenna. The antenna's lower band is formed by a dual-resonant mode mainly contributed by the longer branch strip, while the upper band is formed by three resonant modes contributed respectively by one higher-order resonant mode of the longer branch strip, one resonant mode of the coupled-fed loop antenna alone, and one resonant mode of the shorter branch strip. The antenna's lower and upper bands can therefore cover the desired 698–960 and 1710–2690 MHz bands, respectively. The proposed antenna is suitable to be mounted at the top shielding metal wall of the display ground of the laptop computer and occupies a small volume of 4 × 10 × 75 mm^3 above the top shielding metal wall, which makes it promising to be embedded inside the casing of the laptop computer as an internal antenna. Details of the proposed antenna are studied in the paper.* © 2010 Wiley Periodicals, Inc. Microwave Opt Technol Lett 52:2662–2667, 2010; View this article online at wileyonlinelibrary.com. DOI 10.1002/mop.25556

Key words: *mobile antennas; internal laptop computer antennas; LTE antennas; WWAN antennas; coupled-fed loop antennas*

1. INTRODUCTION

To achieve dual-wideband operation to cover the long-term evolution (LTE) [1]/wireless wide area network (WWAN) [2] operation in the 698–960 MHz band for the LTE700/GSM850/900 operation and the 1710–2690 MHz band for the GSM1800/1900/UMTS/LTE2300/2500 operation is a design challenge for the internal laptop computer antennas. Recently, there have been promising internal laptop computer antennas reported for penta-band WWAN operation in the 824–960 and 1710–2170 MHz bands [3–10]. However, since the required bandwidths for the eight-band LTE/WWAN operation are much wider than the penta-band WWAN operation, especially in the lower band that mainly dominates the required dimensions of the antenna, the promising internal LTE/WWAN laptop computer antennas are still very few in the published papers [11]. In the reported design in Ref. 11, the internal eight-band LTE/WWAN laptop computer antenna occupies a volume of 4 × 10 × 85 mm^3 at the top edge of the display ground to cover the desired 698–960 and 1710–2690 MHz bands. Owing to the continuous requirement in decreasing the size of the internal antennas in the mobile devices, new antenna techniques in achieving smaller size of the internal laptop computer antennas are still very demanding.

In this article, a new antenna structure of internal laptop computer antenna formed by a coupled-fed loop antenna connected with two branch radiators for the eight-band LTE/WWAN operation in the laptop computer is presented. Owing to the proposed new antenna structure, which is different from the reported loop/monopole combo antenna [11] formed by combining a quarter-wavelength printed loop antenna with an internal matching circuit [12, 13] and a printed monopole antenna with an internal distributed inductor [14, 15] for the LTE/WWAN operation, the required size for covering the desired 698–960 and 1710–2690 MHz bands is 4 × 10 × 75 mm^3 only and is smaller than that of the reported antenna in [11]. Details of the proposed antenna are described in this article. The antenna are fabricated and tested, and the results of the fabricated antenna are discussed.

2. PROPOSED ANTENNA

Figure 1 shows the geometry of the proposed coupled-fed loop antenna with branch radiators for the eight-band LTE/WWAN operation in the laptop computer. In the study, the laptop computer is modeled as a display ground and a keyboard ground separated by an angle (α) of 90°. The two grounds are of the same dimensions of 200 × 260 mm^2, which is reasonable for practical laptop computers. The antenna is mounted at the shielding metal wall of width 5 mm and length 260 mm, which is connected to the top edge of the display ground to reduce possible coupling between the antenna and the circuitry on the back side of the laptop display. Also note that since the central region of the top edge of the display is mainly reserved to accommodate the lens of the embedded digital camera, the antenna is mounted along the top shielding metal wall with a spacing of 30 mm to the center line of the display ground.

The major portion of the antenna is printed on a 0.8-mm thick FR4 substrate of width 10 mm and length 75 mm. A 0.2-mm thick metal plate of size 4 × 75 mm^2 is then connected to the printed metal pattern on the FR4 substrate at point D, E, and F. The connected metal plate is orthogonal to the printed metal pattern and parallel to the shielding metal wall. The total volume of the antenna at the shielding metal wall is hence 4 × 10 × 75 mm^3, which is promising to be embedded inside the casing of the practical laptop computer.

The proposed antenna is mainly a coupled-fed loop antenna (path ADEC in the figure) with a longer branch strip (path EFG)

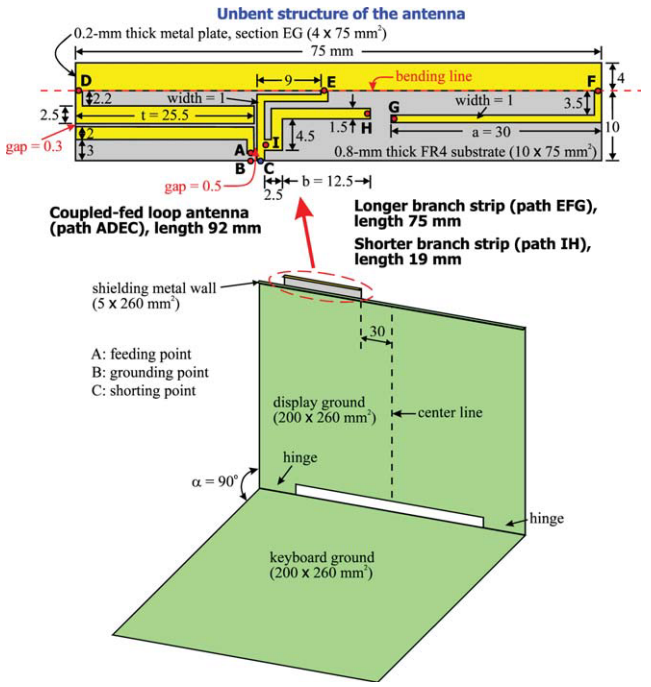

Figure 1 Geometry of the proposed coupled-fed loop antenna with branch radiators for the eight-band LTE/WWAN operation in the laptop computer. [Color figure can be viewed in the online issue, which is available at wileyonlinelibrary.com]

and a shorter branch strip (path IH). The loop antenna has a total length of about 92 mm and is excited capacitively using a coupling feed, which is formed by a feeding strip (width 2 mm and length 25.5 mm) and a coupling strip (width 2.5 mm and length (t) 25.5 mm). By varying the length t of the coupling strip, the capacitive excitation of the loop antenna can be adjusted. With the length t selected to be 25.5 mm, the loop antenna can contribute a resonant mode (0.5-wavelength loop mode) at about 2.4 GHz. Note that point A, the feeding point of the loop antenna, is also the feeding point of the proposed antenna, while point B at the shielding metal wall is the grounding point for a 50-Ω mini coaxial line (not shown in the figure) [10, 11] used to feed the proposed antenna in the experiment. The center conductor and outer grounding sheath of the mini coaxial line are connected respectively to point A and B. Also, point C at the end point of the loop antenna is short-circuited to the shielding metal wall to form the closed loop path.

The longer branch strip connected to the loop antenna at point E results in the formation of a new resonant path including section EC (length about 19 mm) and the longer branch strip (length 75 mm) itself. The new resonant path thus has a total length of about 94 mm, which leads to the generation of a quarter-wavelength resonant mode at about 0.8 GHz and a higher-order resonant mode at about 1.9 GHz. Similarly, the shorter branch strip connected to the loop antenna at point I provides a second new resonant path including section IC and the shorter branch strip. The total length of the second new resonant path is hence about 21 mm, which contributes to a quarter-wavelength resonant mode at about 2.7 GHz. The three resonant modes at about 1.9, 2.4, and 2.7 GHz, which are contributed respectively by the longer branch strip, the loop antenna, and the shorter branch strip, are combined into a wide operating band for the antenna's upper band to cover the desired GSM1800/1900/UMTS/LTE2300/2500 operation (1710–2690 MHz). On the other hand, the resonant mode at about 0.8 GHz contributed by

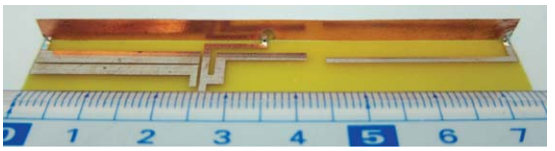

Figure 2 Photo of the fabricated antenna. [Color figure can be viewed in the online issue, which is available at wileyonlinelibrary.com]

the longer branch strip exhibits a dual-resonant property and provides a wide operating band to cover the desired LTE700/GSM850/900 operation (698–960 MHz). The two branch strips connected to the loop antenna hence greatly enhance the bandwidths of the antenna's lower and upper bands, allowing the antenna to cover the eight-band LTE/WWAN operation with a small occupied volume. More detailed operating principle for the proposed antenna is discussed in the next section.

3. RESULTS AND DISCUSSION

The proposed antenna was fabricated and studied. Figure 2 shows the photo of the fabricated antenna. In the experiment, as stated in Section 2, a 50-Ω mini coaxial line (not shown in the figure) aligned along the shielding metal wall is used to feed the antenna. Results of the measured and simulated return loss for the fabricated antenna are shown in the figure. The simulated results are obtained using the Ansoft High Frequency Structure Simulator (HFSS), version 12 [16]. Similar results between the measurement and simulation are observed. Two wide operating bands are obtained for the fabricated antenna. The lower band shows a 3:1 VSWR bandwidth of 302 MHz (670–972 MHz), while that for the upper band is as large as 1210 MHz (1650–2860 MHz). The 3:1 VSWR or 6-dB return-loss bandwidth definition is widely used for the internal WWAN antennas and the LTE antennas as well in the mobile device applications [3–11]. The wide lower and upper bands obtained for the proposed antenna cover the desired eight-band LTE/WWAN operation.

The operating principle of the proposed antenna is analyzed with the aid of Figures 4 and 5. Results of the simulated return loss for the case with a coupled-fed loop antenna only (Ref1), Ref1 connected with a longer branch strip (Ref2), and Ref2 connected with a shorter branch strip (proposed antenna) are shown in Figure 4. The corresponding simulated input impedance for Ref1, Ref2, and proposed antenna is presented in Figure 5.

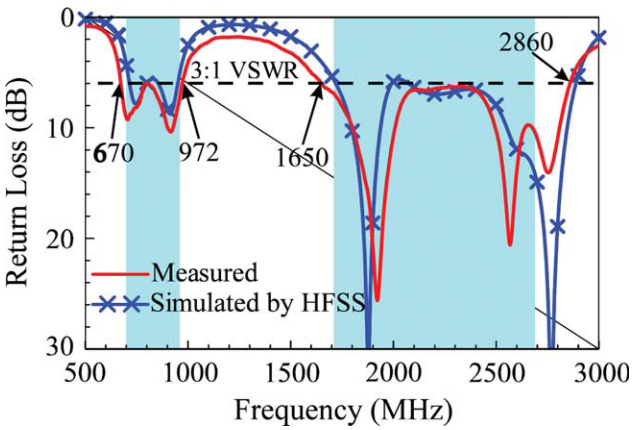

Figure 3 Measured and simulated return loss for the fabricated antenna. [Color figure can be viewed in the online issue, which is available at wileyonlinelibrary.com]

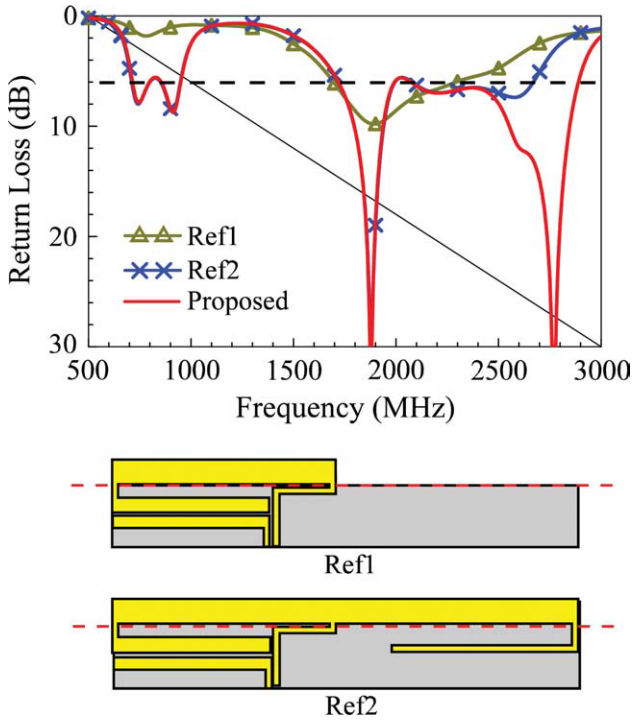

Figure 4 Simulated return loss for the case with a coupled-fed loop antenna only (Ref1), Ref1 connected with a longer branch strip (Ref2), and Ref2 connected with a shorter branch strip (proposed antenna). [Color figure can be viewed in the online issue, which is available at wileyonlinelibrary.com]

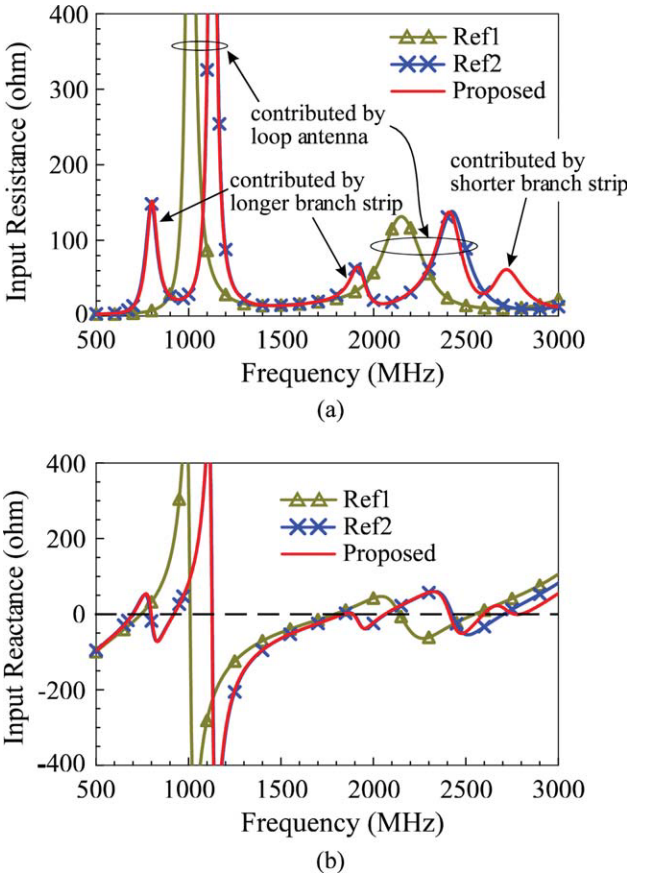

Figure 5 Simulated input impedance for Ref1, Ref2 and proposed antenna studied in Fig. 5. (a) Input resistance. (b) Input reactance. [Color figure can be viewed in the online issue, which is available at wileyonlinelibrary.com]

From the results, it can be concluded that the resonant mode excited at about 2.4 GHz in the proposed antenna is contributed by the loop antenna [Fig. 5(a)]. This 2.4-GHz resonant mode is the 0.5-wavelength loop mode, which is usually excited as the fundamental mode (the lowest mode) of the loop antenna for internal mobile device applications [17–27]. For the resonant mode excited at about 1 GHz as seen in Figure 5, it is also contributed by the loop antenna and is the 0.25-wavelength loop mode. However, this 0.25-wavelength loop antenna [12, 13] shows very high input impedance and results in poor impedance matching or return loss as seen in Figure 4. Both the two loop resonant modes are also seen to be shifted to higher frequencies with the presence of the longer and shorter branch strips.

By comparing Ref1 and Ref2 in Figures 4 and 5, it can be concluded that the resonant modes at about 0.8 and 1.9 GHz is owing to the presence of the longer branch strip. Further, the resonant mode at about 0.8 GHz shows a dual-resonant property (Fig. 4) [28–30] owing to the small values of its input impedance and the close proximity of the excited 0.25-wavelength loop mode, although this loop mode has a very high input impedance level. From the comparison of Ref2 and proposed antenna, an additional resonant mode at about 2.7 GHz is generated owing to the presence of the shorter branch strip. This resonant mode combines the other two modes at about 1.9 and 2.4 GHz to form a very wide operating band for the antenna's upper band.

A parametric study of the proposed antenna is conducted in Figures 6–10. Effects of the width w of the shielding metal wall are analyzed in Figure 6. Simulated return loss for the width w varied from 0 (no shielding metal wall) to 8 mm is presented in the figure. For $w = 0$, wider bandwidth for the antenna's upper band and improved impedance matching for the lower band is seen. For $w = 8$ mm, degraded impedance matching for the lower band is seen. From the results, it indicates that the presence of the shielding metal wall, although it can suppress the possible coupling between the internal antenna and the circuitry on the back side of the laptop display, will cause degraded impedance matching and decreased bandwidth for the internal laptop computer antenna. The presence of the shielding metal wall is hence required to be taken into consideration for the internal laptop computer antenna design.

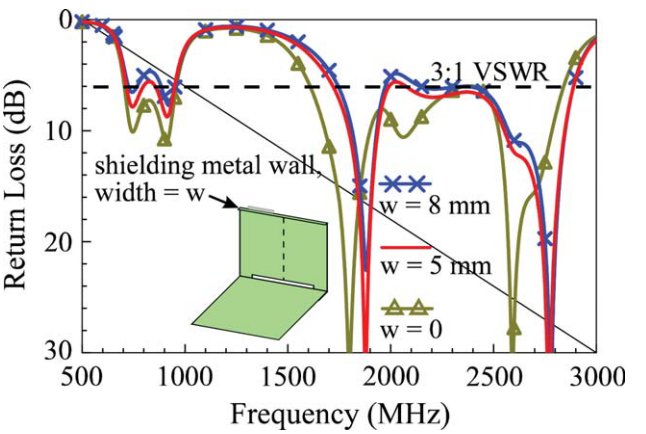

Figure 6 Simulated return loss for the proposed antenna as a function of the width w of the shielding metal wall at the display ground. [Color figure can be viewed in the online issue, which is available at wileyonlinelibrary.com]

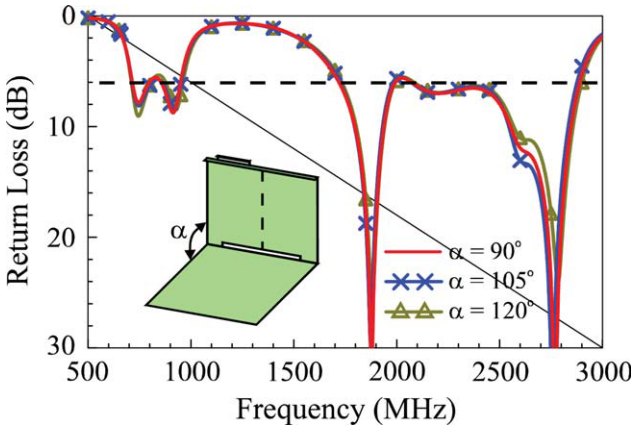

Figure 7 Simulated return loss for the proposed antenna as a function of the angle α between the display ground and the keyboard ground. [Color figure can be viewed in the online issue, which is available at wileyonlinelibrary.com]

Effects of the angle α between the display ground and the keyboard ground are studied in Figure 7. Results of the simulated return loss for the angel α varied from 90 to 105° are presented in Figure 7. Very small variations in the return loss for the three different angles are seen. This is mainly because the display ground alone has a very large size compared to the proposed antenna. Hence, the presence of the keyboard ground and its orientation variations to the display ground will cause small effects on the performances of the proposed antenna.

Figure 8 shows the simulated return loss for the proposed antenna as a function of the length *t* of the coupling strip. Results for the length *t* varied from 19.5 to 25.5 mm are shown. Since the variations in the length *t* will cause large variations in the capacitive coupling of the loop antenna and the two connected branch strips as well, it is no surprise that large variations in the simulated return loss over the antenna's lower and upper bands are seen.

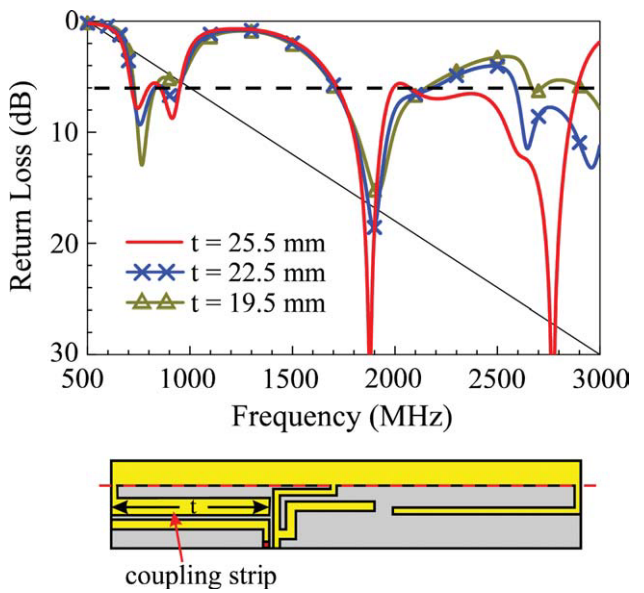

Figure 8 Simulated return loss for the proposed antenna as a function of the length *t* of the coupling strip. Other dimensions are the same as in Figure 1. [Color figure can be viewed in the online issue, which is available at wileyonlinelibrary.com]

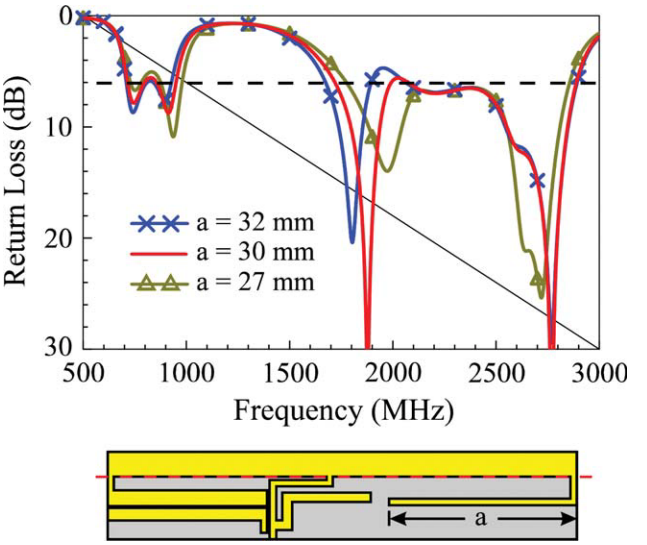

Figure 9 Simulated return loss for the proposed antenna as a function of the length *a* of the end section of the longer branch strip. Other dimensions are the same as in Figure 1. [Color figure can be viewed in the online issue, which is available at wileyonlinelibrary.com]

Figure 9 shows the simulated return loss for the proposed antenna as a function of the length *a* of the end section of the longer branch strip. Results for the length *a* varied from 27 to 32 mm are shown. Small effects on the resonant mode at about 2.4 GHz contributed by the loop antenna are seen. This is reasonable, since the variations in the length *a* do not cause dimensions variations in the coupled-fed loop antenna. On the other hand, large effects on the resonant modes at about 0.8 and 1.9 GHz mainly contributed by the longer branch strip are seen. Some variations in the resonant modes at about 2.7 GHz contributed by the shorter branch strip are also observed. This is largely because the two ends of the longer and shorter branch strips face each other with a small distance. Hence, there exists some coupling between the two branch strips. The impedance matching of the resonant mode contributed by the shorter branch

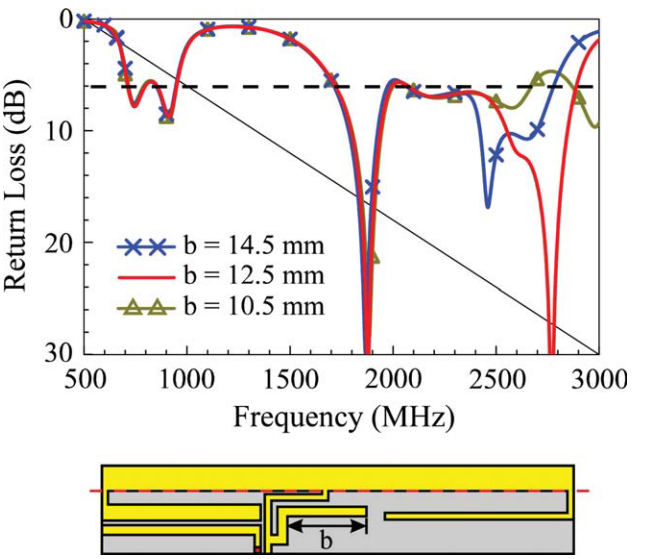

Figure 10 Simulated return loss for the proposed antenna as a function of the length *b* of the end section of shorter branch strip. Other dimensions are the same as in Figure 1. [Color figure can be viewed in the online issue, which is available at wileyonlinelibrary.com]

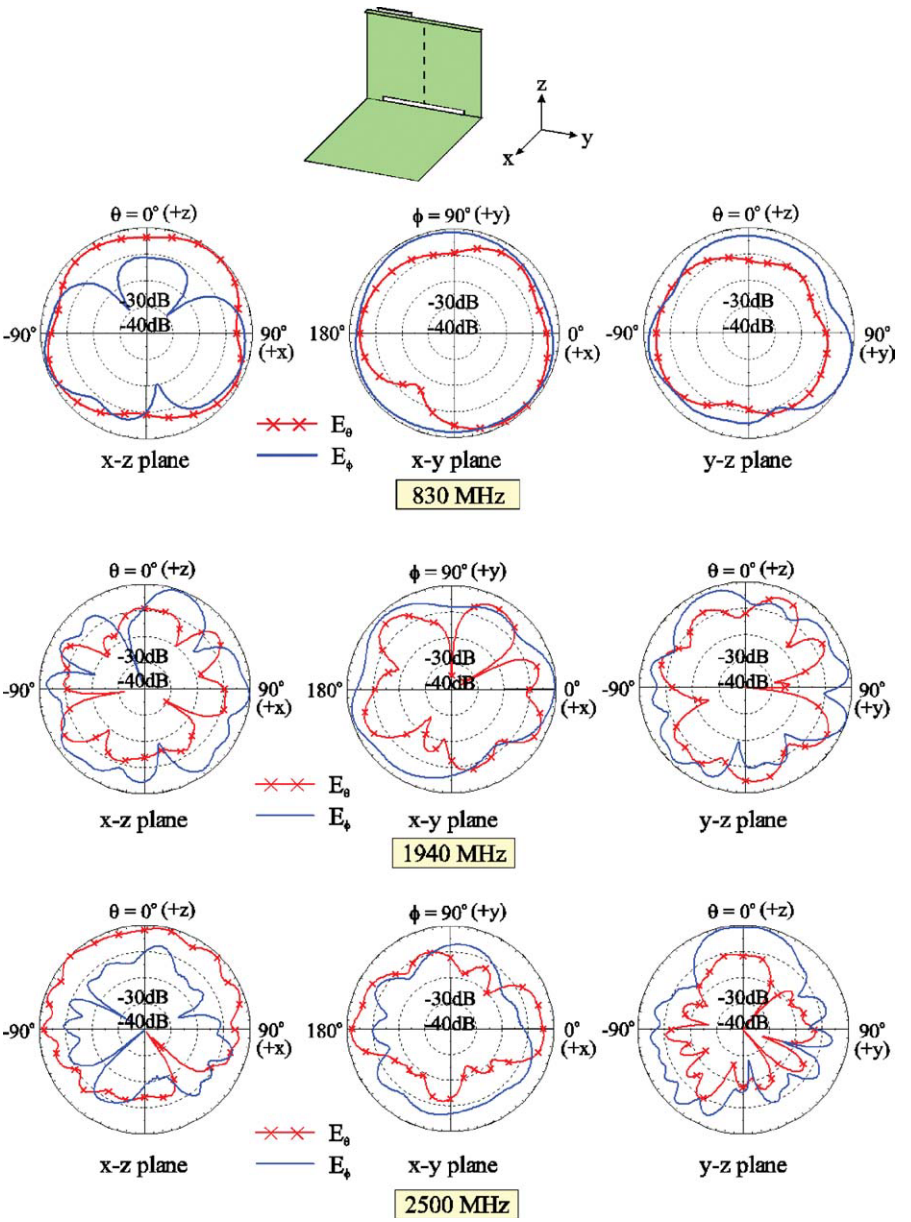

Figure 11 Measured radiation patterns for the proposed antenna. [Color figure can be viewed in the online issue, which is available at wileyonlinelibrary.com]

strip will therefore be affected by the variations in the length a of the end section of the longer branch strip.

Effects of the length b of the end section of the shorter branch strip are studied in Figure 10. Results for the length b varied from 10.5 to 14.5 mm are shown. Large effects on the resonant mode at about 2.7 GHz contributed by the shorter branch strip are seen. This confirms that the resonant mode at about 2.7 GHz is mainly contributed by the shorter branch strip. For the other resonant modes, very small effects are observed.

The measured radiation characteristics of the fabricated antenna are also studied. Figure 11 shows the measured radiation patterns at 830, 1940, and 2500 MHz. At each frequency, the radiation patterns in three principal planes of x-z, x-y, and y-z planes are shown. Comparable E_θ and E_ϕ components are seen. In the azimuthal plane (x-y plane), it is also seen that there are no nulls in the E_θ and E_ϕ components in all the ϕ angles. This is an advantage for practical applications since it can lead to good communication coverage in the azimuthal plane.

Figure 12 shows the measured radiation efficiency for the fabricated antenna. The measured radiation efficiency is about 55–68% and 55–82%, respectively for the lower band [Fig. 12(a)] and the upper band [Fig. 12(b)]. The measured antenna gain varies from about −0.4 to 1.5 dBi for the lower band and 1.0–4.3 dBi for the upper band. The measured radiation characteristics are acceptable for practical laptop computer applications.

4. CONCLUSION

A new internal LTE/WWAN laptop computer antenna to be mounted at the shielding metal wall of the display ground has been proposed. The antenna occupies a volume of 4 × 10 × 75 mm^3 only and provides two wide operating bands (698–960/1710–2690 MHz) to cover the eight-band operation of LTE700/GSM850/900 and GSM1800/1900/UMTS/LTE2300/2500. The dual-wideband operation is obtained by connecting two branch radiators to a coupled-fed loop antenna. The coupling feed in the loop antenna also successfully excites additional resonant

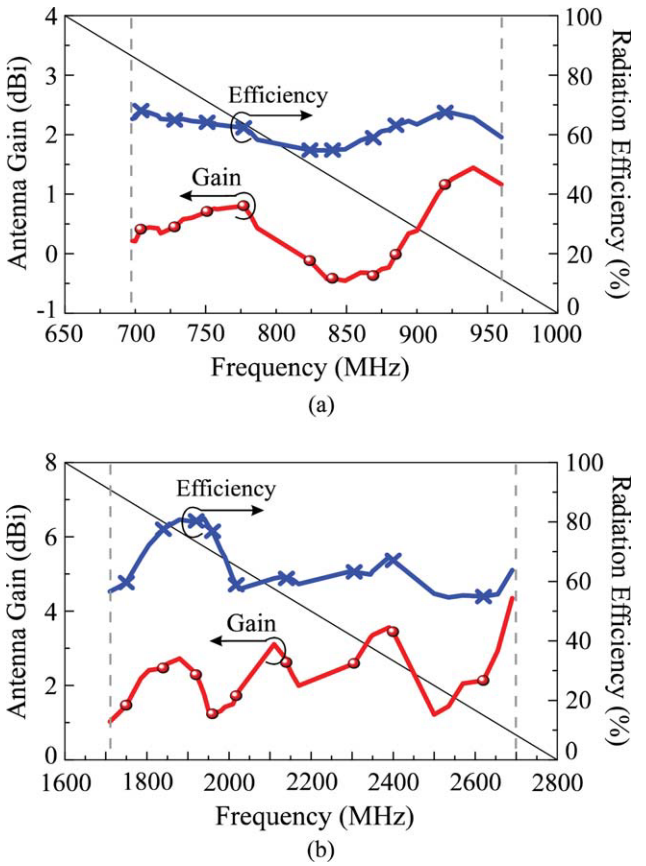

Figure 12 Measured radiation efficiency for the proposed antenna. (a) The lower band. (b) The upper band. [Color figure can be viewed in the online issue, which is available at wileyonlinelibrary.com]

modes which are owing to the presence of the connected branch radiators. The additional resonant modes form the antenna's wide lower band and greatly enhance the bandwidth of the antenna's upper band. Good radiation characteristics over the operating bands have also been observed. The proposed antenna is promising for the LTE/WWAN operation in the laptop computer as an internal antenna.

REFERENCES

1. S. Sesia, I. Toufik, and M. Baker (Eds.), LTE, The UMTS long term evolution: From theory to practice, Wiley, New York, 2009.
2. K.L. Wong, Planar antennas for wireless communications, Wiley, New York, 2003.
3. X. Wang, W. Chen, and Z. Feng, Multiband antenna with parasitic branches for laptop applications, Electron Lett 43 (2007), 1012–1013.
4. C.H. Chang and K.L. Wong, Internal coupled-fed shorted monopole antenna for GSM850/900/1800/1900/UMTS operation in the laptop computer, IEEE Trans Antennas Propag 56 (2008), 3600–3604.
5. K.L. Wong and S.J. Liao, Uniplanar coupled-fed printed PIFA for WWAN operation in the laptop computer, Microwave Opt Technol Lett 51 (2009), 549–554.
6. K.L. Wong and L.C. Lee, Multiband printed monopole slot antenna for WWAN operation in the laptop computer, IEEE Trans Antennas Propag 57 (2009), 324–330.
7. C. Zhang, S. Yang, S. El-Ghazaly, A.E. Fathy, and V.K. Nair, A low-profile branched monopole laptop reconfigurable multiband antenna for wireless applications, IEEE Antennas Wireless Propag Lett 8 (2009), 216–219.
8. K.L. Wong and F.H. Chu, Internal planar WWAN laptop computer antenna using monopole slot elements, Microwave Opt Technol Lett 51 (2009), 1274–1279.
9. C.W. Chiu, Y.J. Chi, and S.M. Deng, An internal multiband antenna for WLAN and WWAN applications, Microwave Opt Technol Lett 51 (2009), 1803–1807.
10. C.T. Lee and K.L. Wong, Study of a uniplanar printed internal WWAN laptop computer antenna including user's hand effects, Microwave Opt Technol Lett 51 (2009), 2341–2346.
11. T.W. Kang and K.L. Wong, Internal printed loop/monopole combo antenna for LTE/GSM/UMTS operation in the laptop computer, Microwave Opt Technol Lett, in press.
12. Y.W. Chi and K.L. Wong, Quarter-wavelength printed loop antenna with an internal printed matching circuit for GSM/DCS/PCS/UMTS operation in the mobile phone, IEEE Trans Antennas Propag 57 (2009), 2541–2547.
13. Y.W. Chi and K.L. Wong, Very-small-size printed loop antenna for GSM/DCS/PCS/UMTS operation in the mobile phone, Microwave Opt Technol Lett 51 (2009), 184–192.
14. C.H. Chang and K.L. Wong, Small-size printed monopole with a printed distributed inductor for penta-band WWAN mobile phone application, Microwave Opt Technol Lett 51 (2009), 2903–2908.
15. T.W. Kang and K.L. Wong, Chip-inductor-embedded small-size printed strip monopole for WWAN operation in the mobile phone, Microwave Opt Technol Lett 51 (2009), 966–971.
16. http://www.ansoft.com/products/hf/hfss/, Ansoft Corporation HFSS.
17. C.A. Balanis, K.D. Katsiba, P.A. Tirkas, and C.R. Birtcher, Loop antenna for mobile and personal communication systems, IEEE Vehicular Technol Conf 2 (1997), 452–454.
18. T. Adachi, A. Hirata, and T. Shiozawa, Folded-loop antennas for handset terminals at the 2.0-GHz band, Microwave Opt Technol Lett 36 (2003), 376–378.
19. B.K. Yu, B. Jung, H.J. Lee, F.J. Harackiewicz, and B. Lee, A folded and bent internal loop antenna for GSM/DCS/PCS operation of mobile handset applications, Microwave Opt Technol Lett 48 (2006), 463–467.
20. B. Jung, H. Rhyu, Y.J. Lee, F.J. Harackiewicz, M.J. Park, and B. Lee, Internal folded loop antenna with tuning notches for GSM/GPS/DCS/PCS mobile handset applications, Microwave Opt Technol Lett 48 (2006), 1501–1504.
21. Y.W. Chi and K.L. Wong, Internal compact dual-band printed loop antenna for mobile phone application, IEEE Trans Antennas Propag 55 (2007), 1457–1462.
22. C.I. Lin and K.L. Wong, Internal meandered loop antenna for GSM/DCS/PCS multiband operation in a mobile phone with the user's hand, Microwave Opt Technol Lett 49 (2007), 759–765.
23. W.Y. Li and K.L. Wong, Surface-mount loop antenna for AMPS/GSM/DCS/PCS operation in the PDA phone, Microwave Opt Technol Lett 49 (2007), 2250–2254.
24. W.Y. Li and K.L. Wong, Internal printed loop-type mobile phone antenna for penta-band operation, Microwave Opt Technol Lett 49 (2007), 2595–2599.
25. C.I. Lin and K.L. Wong, Internal multiband loop antenna for GSM/DCS/PCS/UMTS operation in the small-size mobile phone, Microwave Opt Technol Lett 50 (2008), 1279–1285.
26. K.L. Wong and C.H. Huang, Printed loop antenna with a perpendicular feed for penta-band mobile phone application, IEEE Trans Antennas Propag 56 (2008), 2138–2141.
27. M.R. Hsu and K.L. Wong, Seven-band folded-loop chip antenna for WWAN/WLAN/WiMAX operation in the mobile phone, Microwave Opt Technol Lett 51 (2009), 543–549.
28. K.L. Wong and C.H. Huang, Bandwidth-enhanced internal PIFA with a coupling feed for quad-band operation in the mobile phone, Microwave Opt Technol Lett 50 (2008), 683–687.
29. K.L. Wong and C.H. Huang, Printed PIFA with a coplanar coupling feed for penta-band operation in the mobile phone, Microwave Opt Technol Lett 50 (2008), 3181–3186.
30. C.H. Chang, K.L. Wong, and J.S. Row, Coupled-fed small-size PIFA for penta-band folder-type mobile phone application, Microwave Opt Technol Lett 51 (2009), 18–23.